Hindawi
Advances in Civil Engineering
Volume 2021, Article ID 9565730, 15 pages
https://doi.org/10.1155/2021/9565730

Research Article

Dynamic Characteristics of a Double-Pylon Cable-Stayed Bridge with Steel Truss Girder and Single-Cable Plane

Yong Zeng,[1,2] **Yutong Zeng**,[1,2] **Hao Yu**,[1,2] **Yujie Tan**,[1,2] **Hongmei Tan**,[1,2] **and Huijun Zheng**[3]

[1]*State Key Laboratory of Mountain Bridge and Tunnel Engineering, Chongqing Jiaotong University, Chongqing 400074, China*
[2]*Mountain Bridge and Materials Engineering Research Center of Ministry of Education, Chongqing Jiaotong University, Chongqing 400074, China*
[3]*Hebei Petroleum University of Technology, Hebei 067000, China*

Correspondence should be addressed to Yong Zeng; yongzeng@cqjtu.edu.cn

Received 28 August 2021; Accepted 3 December 2021; Published 16 December 2021

Academic Editor: Iman Mansouri

The dynamic characteristics are closely linked to the seismic stability and wind-resistant of the bridge. But different bridge types have different dynamic characteristics. In order to study the dynamic characteristics of a double-pylon cable-stayed bridge with a single-cable plane and steel truss girder whose main span is the longest in the world, the dynamic load test was done, and the finite element and the subspace iteration methods were used to analyze the vibration mode of the bridge. The influence of different structural parameters on the dynamic characteristics of the bridge was analyzed. The changed structural parameters are cable layout, stiffness of steel truss girder, stiffness of stayed cables, stiffness of pylons, the concentration of dead load, number and location of auxiliary piers, and structural system. The results show that the bending and torsion resistance of the double-pylon cable-stayed bridge with a single-cable plane and steel truss girder is weak. The torsional stiffness of the cable-stayed bridge with a double-cable plane is stronger than that of the cable-stayed bridge with a single-cable plane. The seismic stability and wind-resistant of the bridge can be improved by using light dead load, improving the stiffness of pylon and girder, and adding auxiliary piers scientifically. However, the change of cable stiffness has a complex influence on the dynamic characteristics of the bridge. The conclusion can offer references for the construction, maintenance, and design of the same type of bridges.

1. Introduction

Nowadays, more and more beautiful bridges are being built. A beautifully shaped bridge can become a landmark of a city or even a symbol of urban culture. The double-pylon cable-stayed bridge with single-cable plane and steel truss girder has not only strong performance but also a beautiful appearance. It is a functional artwork integrated with the environment. Artworks are usually kept in museums and hardly suffer from any natural disasters. However, modern bridges, which are functional works of art, need to withstand earthquakes, strong wind, and other natural disasters. The dynamic characteristics of the bridge are closely related to the seismic stability and wind-resistant of the bridge [1, 2]. Moreover, the dynamic characteristics can also reflect the stability of the traffic and detect the health status of the bridge [3, 4]. The dynamic characteristics of each bridge type are unique and need to be studied separately. The dynamic characteristics of the same type of bridge are similar. If the dynamic characteristics of a certain type of bridge can be determined, it can offer references for similar bridges [5]. The structure of the double-pylon cable-stayed bridge with a single-cable plane and steel truss girder is complex and its dynamic characteristics are not clear. Therefore, it is necessary to study its dynamic characteristics, which are of great engineering significance.

A study of the dynamic characteristics of cable-stayed bridges can reveal how the bridges react under various dynamic excitation [6, 7]. The dynamic characteristics of the bridge can be measured by field tests or by finite element method analysis. Field measurement is usually used to test the real bridge, and the structural parameters cannot be changed. However, the finite element method analysis can change different structural parameters to find a method to optimize the dynamic characteristics of a certain bridge type [8–10]. If the modeling is accurate and the boundary conditions are simulated properly, there is little difference between the finite element method and the field measurement results. Subspace iterative method is one of the methods to analyze the dynamic characteristics of bridges, which has enough accuracy [11–14]. Changing some structural parameters of the bridge may enhance its dynamic characteristics [15, 16]. The dynamic characteristics of a long-span bridge will change with the change of stiffness of each component and the change of constraint between the pylon and girder [17, 18]. The change of boundary conditions also results in the change of dynamic characteristics of the bridge [19]. The influence of dead load concentration on the dynamic characteristics of the bridge cannot be ignored. For a long-span cable-stayed bridge, it is necessary to verify the reliability of the dynamic response of heavy-haul trains resting on the bridge [20]. Auxiliary piers also have a certain influence on the dynamic characteristics of the cable-stayed bridge [21]. Zhou et al. [22] investigated the dynamic characteristics of an extrawide concrete self-anchored suspension bridge. The width of this bridge is very large, and its dynamic characteristics are worth studying. Ventura et al. [23] studied the dynamic characteristics of the Colquitz River Bridge by full-scale testing. Their research was later used by bridge owners to assess the expected response of bridges during earthquakes. Roy and Dash [24] studied the dynamic behavior of the multispan continuous girder bridge. Although the multispan continuous girder bridge is not a new type of bridge, many bridges of this type are built. The study of its dynamic characteristics is still valuable. Xie et al. [25] investigated the dynamic characteristics of a long-span cable-stayed bridge with CFRP cables. It is found that CFRP has excellent mechanical properties and can be used in long-span cable-stayed bridges. Casalegno and Russo [26] also studied the dynamic characteristics of the bridge using new material. The dynamic characteristics of many other bridges have been studied, including ordinary cable-stayed bridges, suspension bridges, and continuous rigid frame bridges [27–37]. These studies mainly focus on the dynamic characteristics of widely used general bridges and new bridges. The studies of the dynamic characteristics of the widely used general bridges are helpful to the formulation of the code. The research on the dynamic characteristics of the new bridges can provide a reference for similar bridges to be built in the future. The double-pylon cable-stayed bridge with steel truss girder and a single-cable plane is a new type of bridge, and its dynamic characteristics are is worth research. However, there are few studies on the influence of different stayed cable surface arrangements, girder stiffness, cable stiffness, pylon stiffness, the concentration of the dead load, number of auxiliary piers, and structural system on the dynamic characteristics of the double-pylon cable-stayed bridge with a single-cable plane and steel truss girder.

A double-pylon cable-stayed bridge with a single-cable plane and steel truss girder was taken as an example. The dynamic load test was done to verify the FE model, and the finite element method was adopted. The influence of different stayed cable surface arrangements, girder stiffness, cable stiffness, pylon stiffness, the concentration of the dead load, number of auxiliary piers, and structural system on the dynamic characteristics of a double-pylon cable-stayed bridge with single-cable plane and steel truss girder was analyzed. The dynamic characteristics of the same type of long-span bridges are similar, so the conclusions of this paper can be referenced by similar bridges and be of universal significance. This paper is a supplement to the study of the dynamic characteristics of the double-pylon cable-stayed bridge with a single-cable plane and steel truss girder, which can offer references for the construction, maintenance, and design of the same type of bridges and offer some new ideas for the study of the dynamic characteristics of other types of bridge.

2. Dynamic Analysis Theory Based on Finite Element Method

2.1. Characteristic Equations. When a bridge is in free vibration, the vibration equation of the multifree vibrating system under the condition of neglecting damping is as follows:

$$\left[K^{*}-\omega^{2}M^{*}\right]\{a\}=0, \tag{1}$$

where K is generalized stiffness matrix; M is generalized mass matrix; W is free vibration circle frequency; a is a characteristic vector.

Equation (1) can be deduced by the Cramer rule. The characteristic equation is as follows:

$$\left|K^{*}-\omega^{2}M^{*}\right|=0. \tag{2}$$

2.2. Dynamic Characteristic Analysis Process. The subspace iteration method was used to analyze the dynamic characteristics of the double-pylon cable-stayed bridge with a single-cable plane and steel truss girder. Subspace iterative method is one of the methods to analyze the dynamic characteristics of bridges, which has enough accuracy. The first n-order frequencies and mode shapes of the double-pylon cable-stayed bridge with single-cable plane and steel truss girder were analyzed by using the subspace iteration method. The analysis process is as follows:

(1) Based on the finite element method, the whole process from the beginning of construction to the completion of the double-pylon cable-stayed bridge with a single-cable plane and steel truss girder was calculated. Based on the bridge state, the total stiffness matrix and the total mass matrix were obtained.

(2) The formula, $D=K^{-1}M$, was used to obtain the dynamic matrix of the system D.

(3) After the assumption of n linearly independent normalized modes is selected, they were arranged into an $n\times n$-order matrix $A_0=[\psi_1\psi_2\cdots\psi_n]$.

(4) Each array was normalized to obtain $\psi_1 = DA_0$. After further analysis, the generalized stiffness matrix $K^* = \psi_I^T K \psi_1$ and the generalized mass matrix $M^* = \psi_I^T M \psi_1$ were obtained.

(5) After the equation $K^* a - \omega^2 M^* a = 0$ was converted to $|K^* - \omega^2 M^*| = 0$, the first n-order frequency $\omega_1, \omega_2, \ldots, \omega_n$ and the corresponding eigenvector $a^1, a^2, \ldots, a^n$ were calculated.

(6) Inequality $\|a - I\| < \xi$, where I is the unit vector and ξ is the minimum tolerance, needs to be judged. If the inequality is true, the matrix composed of the first n modes is $A_1 = \phi_1^T [a^1 a^2 \ldots a^n]$ and the first n frequencies are $\omega_1, \omega_2, \ldots, \omega_n$. If not, go back to step (4) and continue with the following steps, instead.

3. Bridge Description

A double-pylon cable-stayed bridge with a single-cable plane and steel truss girder is in Chongqing, China, whose span arrangement is 225.5 m + 445 m (main span) + 190.5 m. Its main span is the longest in the world, and the bridge system is semifloating. Compressive bearings are set between girders, pylons, and platforms. The side span's bearings on both sides are longitudinally free, one pylon is longitudinally restrained, and the other pylon is longitudinally free. The bridge is shown in Figure 1.

The height of the pylons on both sides is 162 m and 172 m, and the material is C50 concrete. As shown in Figure 2, the main girder is arranged with a double-layer steel truss, whose height span ratio is about 1/38. The lower layer is the railway and the upper layer is the highway. Both the upper and lower decks are orthogonal special-shaped decks with a width from 24.500 to 36.990 m due to different functions. The parallel steel strand is selected as the stayed cable; the material is Strand1860. The main span from 400 to 500 m is the economic span range of a double-pylon cable-stayed bridge with a single-cable plane and steel truss girder. The main spans of most similar bridges in the world are concentrated in 400–500 m. The dynamic characteristics of the same type of long-span bridges are similar, so this bridge is a very suitable choice, and the conclusions obtained have the value of promotion. The physical properties of the bridge materials are listed in Table 1.

The bridge in this paper was the first bridge in the world to adopt a cable anchor girder fixed structure, and the world records when the bridge was completed are as follows:

(1) The span of the same type of bridge was the longest in the world.

(2) The anchorage form of cable and girder was first used in the world.

(3) The tonnage of the cable pylon anchor was the biggest in the world.

(4) The sparse cable scheme was adopted. There are only 36 stayed cables in the whole bridge. The single-cable is made up of 139 strands of parallel steel strands. The steel strands of stayed cables are about 980 tons. The tonnage of cables is the biggest in the world.

(5) The large tonnage bearing under the main pylon is supported by a corbel, which was the largest tonnage in the world.

4. Finite Element Simulation

Several finite element models of bridges with different structural parameters were established. The model with all construction completed and unchanged parameters has a total of 17846 nodes and 30128 elements with sufficient accuracy. The pylon and main girder were simulated by beam element, and the cable was simulated by tension only element. In order to accurately reflect the stress situation of the pylons, the section characteristics of each component were selected according to the actual size of the structure. All construction stages (62 in total) were considered, and the geometric nonlinear effect was considered in the modeling. The subspace iteration method was adopted to realize the analysis and research on the bridge vibration mode. Different structural parameters were changed, and several finite element models were established. Except for the change of cable plane layout, other parameters' changes do not change the structure appearance. The finite element model is shown in Figure 3, and the boundary conditions are listed in Table 2.

5. Dynamic Load Test

There are two layers in the steel truss girder, forming a double-layer bridge deck. When secondary dead load had not been laid on the lower deck, the dynamic load test was done on the double-pylon cable-stayed bridge with steel truss girder and single-cable plane. The random vibration method was used for the test and there was no traffic load on the bridge deck during the test. The bridge would vibrate slightly when the water strikes the pier or the wind blows to the bridge. Then, the dynamic characteristics of the bridge could be measured. That is the random vibration method. The advantage of this method is that the experimental process is simple, but the disadvantage is that it can only test the frequencies of the first few modes.

5.1. Introduction of the Test. When secondary dead load had not been laid on the lower deck, the dynamic load test was done on the double-pylon cable-stayed bridge with steel truss girder and single-cable plane by the random vibration method. As shown in Figure 4, some pick-up instruments were installed at the key parts of the bridge. When the bridge vibrates, the sensor will record the amplitude and phase of each measurement point. The modal frequency can be obtained by comparing the amplitude and phase of each measuring point.

A total of 28 pick-up instruments were installed on the bridge, 26 on the steel truss girder, and two on the pylons. The type 941-B longitudinal pulse acceleration sensors and 991-B transverse pulse acceleration sensors were selected for the pick-up instruments, and the amplifiers were set at the same time. The amplifier can amplify the collected vibration signal and transmit it to the computer.

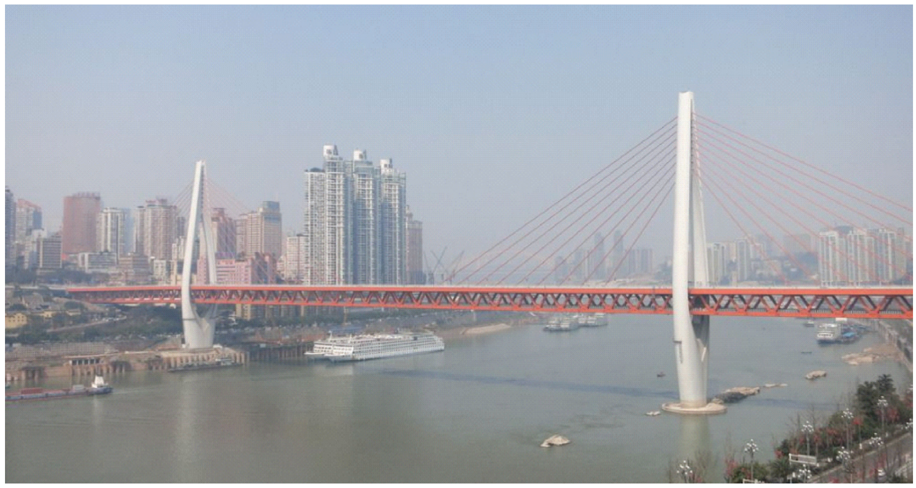

Figure 1: A double-pylon cable-stayed bridge with a single-cable plane and steel truss girder.

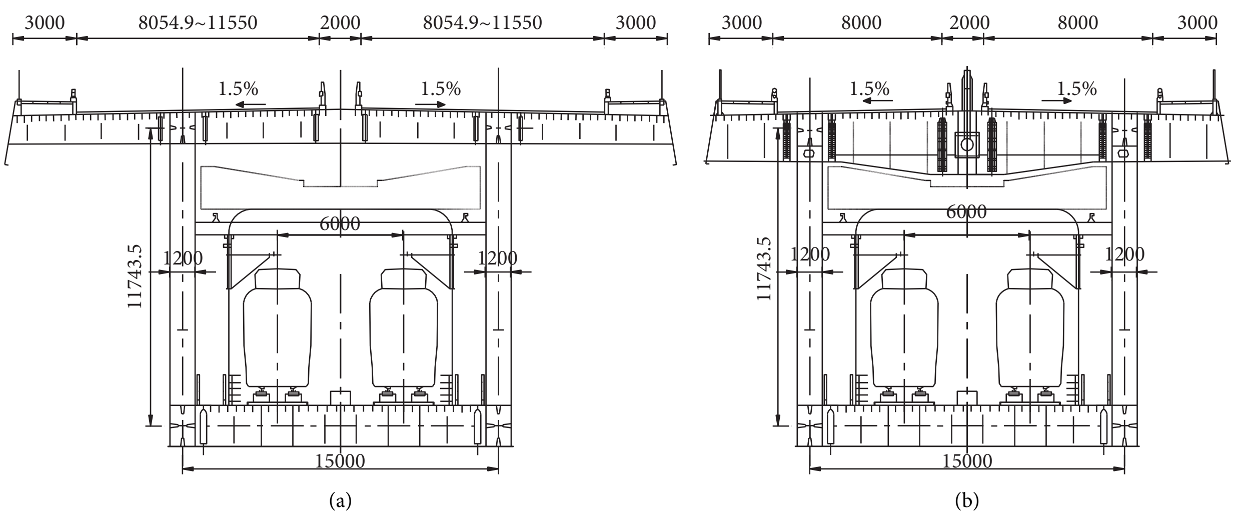

Figure 2: Control section diagram of main girder/mm. (a) Section of the main girder. (b) Section of main girder cable zone.

Table 1: Physical properties of main materials.

Type	Components	Elastic modulus (E/GPa)	Poisson's ratio	Linear expansion coefficient (10–5°C)
C50	Pylon	34.5	0.2	1.0
Q345	Girder	206.0	0.3	1.2
Strand1860	Stayed cables	195.0	0.3	1.2

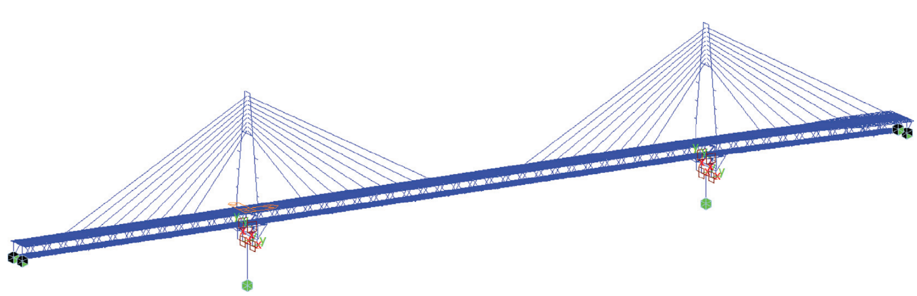

Figure 3: Finite element model of the double-pylon cable-stayed bridge with a single-cable plane and steel truss girder.

Table 2: Boundary conditions of FE model.

Structural parts		Ux	Uy	Uz	ROTx	ROTy	ROTz
Abutment A0	Upstream	0	1	1	0	0	0
	Downstream	0	0	1	0	0	0
Bottom of pylon P1	Upstream	1	1	1	1	1	1
	Downstream	1	1	1	1	1	1
Connection of pylon P1 and girder	Upstream	1	1	1	0	0	0
	Downstream	1	0	1	0	0	0
Bottom of pylon P2	Upstream	1	1	1	1	1	1
	Downstream	1	1	1	1	1	1
Connection of pylon P2 and girder	Upstream	0	1	1	0	0	0
	Downstream	0	0	1	0	0	0
Pier P3	Upstream	0	1	1	0	0	0
	Downstream	0	0	1	0	0	0

Note. 0 for no; 1 for yes.

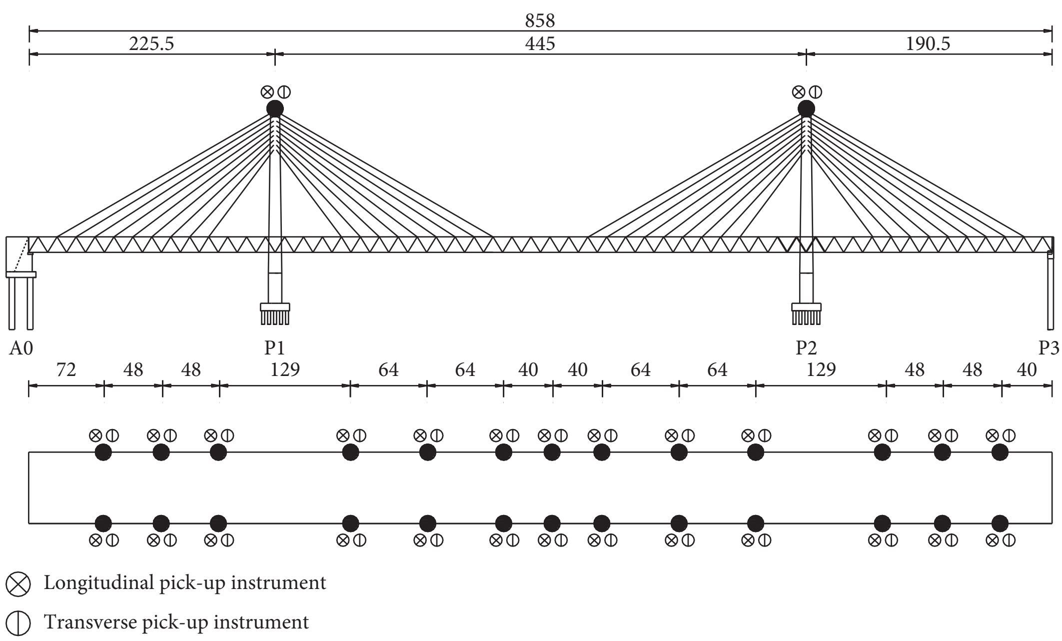

Figure 4: The position of the pick-up instruments on the bridge.

5.2. Comparison of the Results. During the dynamic load test of the bridge, the secondary dead load had not been laid on the lower deck. So, the dynamic characteristics of the two FE models were calculated. Mode 1 is the FE model without secondary dead load on the lower deck, and mode 2 is the FE bridge model whose secondary dead load has been laid on the lower deck and all construction processes have been completed. The random vibration method was used for the dynamic load test. During the test, there were no traffic loads on the bridge deck and no other irregular vibration sources around the bridge site. Dynamic loads were random wind load, water flow load, and other random loads at the bridge site. Because the random vibration method was used for the dynamic load test, the number of vibration modes is less, only the first five modes. The results are listed in Table 3.

During the dynamic load test of the bridge, the secondary dead load had not been laid on the lower deck and the FE model 1 simulates the bridge at that moment. The FE model 2 simulates a fully completed bridge. Because the modeling is accurate and the boundary simulation is correct, the frequencies calculated by the FE model 1 are close to the measured frequencies. For the first five modes, the frequencies calculated by the FE model 1 are slightly higher than the calculated frequencies. During the design of the bridge, the structure would be checked. The structure would not be built until it has been proved safe. The measured frequencies of the bridge are higher than the calculated frequencies, indicating that the stiffness of the bridge is large enough. When secondary dead load laying is completed, the first five modes' frequencies decrease. It conforms to the changing law of the dynamic characteristics of the bridge. In a word, the comparison between measured and calculated values shows that the FE model modeling is accurate and the boundary simulation is correct. The model can be used for subsequent analysis.

Table 3: The comparison between measured frequencies and calculated frequencies.

Mode number	Measured frequencies (Hz)	Calculated frequencies 1 (Hz)	Calculated frequencies 2 (Hz)	Mode shape
1	0.35	0.32	0.24	The 1st-order cross bending of the main span of the girder
2	0.43	0.38	0.31	The 1st-order symmetrical vertical bending of the girder
3	0.69	0.53	0.47	The 2nd-order symmetrical vertical bending of the girder
4	0.73	0.63	0.58	The bending torsion-coupling of the left span of the girder
5	0.91	0.73	0.61	The 1st-order symmetrical bending of the girder

Note. Calculated frequencies 1, calculated by the FE model 1; calculated frequencies 2, calculated by the FE model 2.

6. Analysis of Dynamic Characteristic Analysis Based on Variable Parameters

6.1. Influence of Cable Layout on Dynamic Characteristics. When the bridge was in operation, the secondary dead load had been laid on the lower deck. Therefore, all models used in this chapter are models that have completed all construction. Usually, the study of bridge dynamic characteristics mainly focuses on the first 10 modes, because they are representative and easy to occur in reality. As shown in Table 4, in order to study the influence of the cable plane layout on the dynamic characteristics of the steel truss cable-stayed bridge, the first 12 modes of the cable-stayed bridge with a single-cable plane and the cable-stayed bridge with a double-cable plane were compared. As shown in Figure 5, some modes' shapes of the two bridge types with different cable layouts are compared intuitively. In Figure 5, except for the 1st mode, other mode shapes of the two bridge types are different.

From the analysis of Table 4 and Figure 5, the conclusions are as follows:

(1) For the first five modes, the vibration frequency and period of the cable-stayed bridge with a single-cable plane and the cable-stayed bridge with a double-cable plane are different, but the mode shapes are consistent. When the mode shape is bending torsion-coupling (the 4th-order mode), the frequency of the cable-stayed bridge with a double-cable plane is higher than that of the cable-stayed bridge with a single-cable plane, because the cables of the cable-stayed bridge with a single-cable plane cannot bear the torsion caused by eccentric load and the double-cable plane can enhance the torsional stiffness of cable-stayed bridge. The fundamental frequency of the original structure is 0.244 Hz, and the shape of the 1st-order mode is the first-order transverse bending of the middle span of the main girder, which is the basic mode of the bridge, indicating that the lateral bending stiffness of the double-pylon cable-stayed bridge with single-cable plane and steel truss girder is small. The shape of the 2nd-order mode is the 1st-order symmetrical vertical bending, and the mode shape appears earlier, which proves that the bridge has low longitudinal flexural rigidity and low transverse and longitudinal flexural rigidity. The wind-resistant of the bridge is weak. The shape of the 4th-order mode is the coupling of bending and torsion of the girder. The bending and torsion capacity of the bridge is relatively balanced and weak, which is unfavorable to the wind-resistant of the bridge.

(2) For the 6th-order mode to the 12th-order mode, the frequencies of the cable-stayed bridge with a double-cable plane are greater than those of the cable-stayed bridge with a single-cable plane. From the 6th-order mode to the 9th-order mode, the mode shapes are different. At the 6th-order mode, the 3rd-order symmetrical vertical bending of the main girder of the cable-stayed bridge with a single-cable plane appears, but the 2nd-order symmetrical vertical bending mode of the main girder of the cable-stayed bridge with a double-cable plane appears. At the 7th-order mode and the 9th-order mode, obvious bending torsion-coupling mode of the main girder of the cable-stayed bridge with single-cable plane appears, but slight bending torsion-coupling mode of the main girder of the cable-stayed bridge with a double-cable plane appears. From the 7th-order mode to the 9th-order mode, bending torsion coupled vibration modes appear. The torsion degree of the cable-stayed bridge with a single-cable plane is larger than that of the cable-stayed bridge with a double-cable plane, which proves that the double-cable plane arrangement can improve the torsional characteristics of steel truss girder cable-stayed bridge. At the 10th-order mode and the 12th-order mode, the girder symmetrical vertical of the main span appears. At the 11th-order mode, obvious torsion of the main span of the girder appears. But the double-cable plane only increases the frequency of the mode, and the mode shape is not changed.

(3) There is no pure torsional mode in the first 12 modes; only the coupled mode of bending and torsion is found, which further shows that the bending and torsion capacity of the bridge is equal and weak. This cable-stayed bridge with a single-cable plane and

Table 4: Main vibration mode characteristics.

Mode number	Bridge type	Frequencies (Hz)	Mode shape
1	S	0.244	The 1st-order cross bending of the main span of the girder
	D	0.243	The 1st-order cross bending of the main span of the girder
2	S	0.306	The 1st-order symmetrical vertical bending of the girder
	D	0.325	The 1st-order symmetrical vertical bending of the girder
3	S	0.467	The 2nd-order symmetrical vertical bending of the girder
	D	0.472	The 2nd-order symmetrical vertical bending of the girder
4	S	0.581	The bending torsion-coupling of the left span of the girder
	D	0.584	The bending torsion-coupling of the left span of the girder
5	S	0.612	The 1st-order symmetrical bending of the girder
	D	0.608	The 1st-order symmetrical bending of the girder
6	S	0.656	The 3rd-order symmetrical vertical bending of the girder
	D	0.661	The 2nd-order symmetrical vertical bending of the girder
7	S	0.671	The obvious bending torsion-coupling of the girder
	D	0.673	The slight bending torsion-coupling of the girder
8	S	0.716	The bending torsion-coupling of the main and right span of the girder
	D	0.718	The bending torsion-coupling of the right span of the girder
9	S	0.758	The obvious bending torsion-coupling of the girder
	D	0.763	The slight bending torsion-coupling of the girder
10	S	0.774	The 4th-order symmetrical vertical bending of the girder
	D	0.822	The 4th-order symmetrical vertical bending of the girder
11	S	0.830	The obvious bending torsion-coupling of the main span of the girder
	D	0.919	The obvious bending torsion-coupling of the main span of the girder
12	S	0.946	The 5th-order symmetrical vertical bending of the girder
	D	1.006	The 5th-order symmetrical vertical bending of the girder

Note. S, cable-stayed bridge with a single-cable plane; D, cable-stayed bridge with a double-cable plane.

steel truss girder double-pylon belongs to the semifloating system. The overall bridge is relatively flexible which is conducive to reducing the seismic response. However, from the vibration mode characteristics, the design of a single-cable plane makes the bridge have weak torsional stiffness, which is extremely unfavorable to the wind-resistant. By changing the single-cable plane layout to the double-cable plane layout, the torsional stiffness of the double-pylon cable-stayed bridge with steel truss girder is improved, which can avoid the occurrence of bending and torsion-coupling mode to a certain extent and enhance the wind resistance of the bridge.

6.2. Influence of Other Structural Parameters on Dynamic Characteristics. In order to find measures to improve the wind resistance of a double-pylon cable-stayed bridge with a single-cable and steel truss girder and to maintain its good seismic resistance, the influence of different girder stiffness, cable stiffness, pylon stiffness, the concentration of the dead load, number of auxiliary piers, and structural system on the dynamic characteristics of the double-pylon cable-stayed bridge with a single-cable plane and steel truss girder was analyzed. In order to study the dynamic characteristics of the bridge more precisely, it is divided into two types: bending mode and bending torsion-coupling mode. The first 12 modes are represented by f_1 to f_{12}. The bending mode includes f_1, f_2, f_3, f_4, f_5, f_{10}, and f_{12}, respectively. The bending torsion-coupling mode includes f_6, f_7, f_8, f_9, and f_{11}, respectively.

6.2.1. The Stiffness of Steel Truss Girder. As shown in Figure 6, the stiffness of other components is kept unchanged, the stiffness change coefficient of the girder is set to 0.6, 0.8, 1.2, 1.4, and 1.6, and the bending modes and bending torsion-coupling modes are compared and studied. It is found that the change of the stiffness of the main girder will not affect the mode shape of the bridge.

It can be seen from Figure 6, with the stiffness coefficient of the girder rising from 0.6 to 1.6, the frequency of the first 12 modes of the bridge shows an upward trend. Although they are all rising, it is obvious that the frequency rise of bending mode and bending torsion-coupling mode is different from the rising rate. For bending mode, when the stiffness coefficient increases from 0.6 to 1.6, the maximum rising rate is the fundamental frequency, that is, the frequency of the 1st-order mode (f_1) reaches 60.7%, and the frequency of the 3rd-order mode (f_3) has the smallest rising rate, which is 23.1%. For the 1st-order mode, when the coefficient increases from 0.6 to 1.6, although it only increases by 0.114 Hz, the rising rate is the largest due to its low frequency. When the stiffness of the girder is increased, the bending mode frequency increases, which indicates that the bending capacity of the bridge can be enhanced by increasing the stiffness of the girder. For bending torsion-coupling mode, when the stiffness coefficient increases from

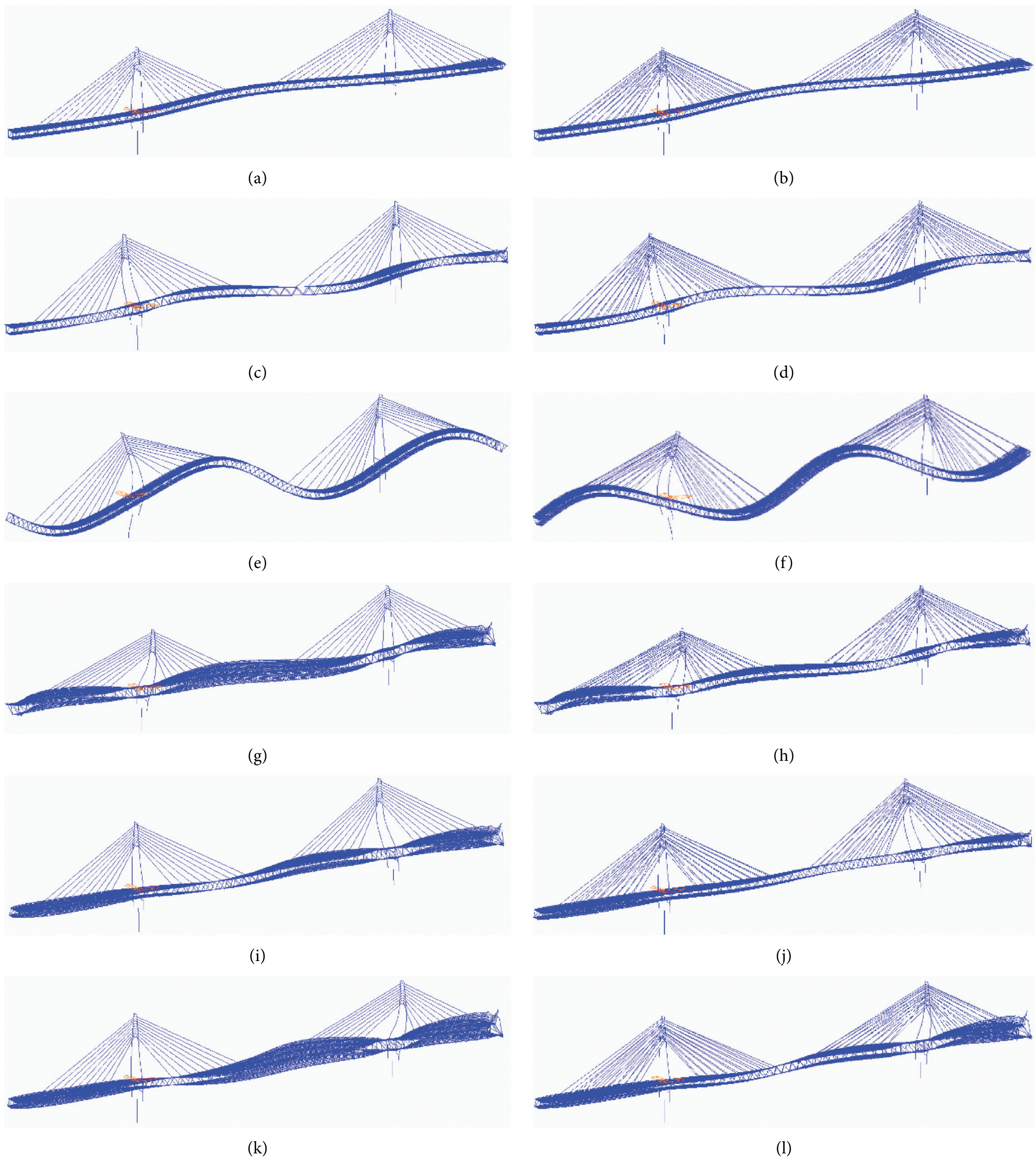

Figure 5: Some vibration modes of two bridges with different cable plane arrangements. (a) The 1st-order mode of the cable-stayed bridge with a single-cable plane. (b) The 1st-order mode of the cable-stayed bridge with a double-cable plane. (c) The 5th-order mode of the cable-stayed bridge with a single-cable plane. (d) The 5th-order mode of the cable-stayed bridge with a double-cable plane. (e) The 6th-order mode of the cable-stayed bridge with a single-cable plane. (f) The 6th-order mode of the cable-stayed bridge with a single double plane. (g) The 7th-order mode of the cable-stayed bridge with a single-cable plane. (h) The 7th-order mode of the cable-stayed bridge with a double-cable plane. (i) The 8th-order mode of the cable-stayed bridge with a single-cable plan. (j) The 8th-order mode of the cable-stayed bridge with a double-cable plane. (k) The 9th-order mode of the cable-stayed bridge with a single-cable plane. (l) The 9th-order mode of the cable-stayed bridge with a double-cable plane.

0.6 to 1.6, the frequency of the 11th-order mode f_{11} reaches 60.0%, and the frequency of the 7th-order mode f_7 has the smallest rising rate, which is 26.9%. Due to the large cardinality of the 11th-order mode itself, the frequency of the girder increases by 0.391 Hz when the stiffness coefficient increases from 0.6 to 1.6, which is far greater than that of the

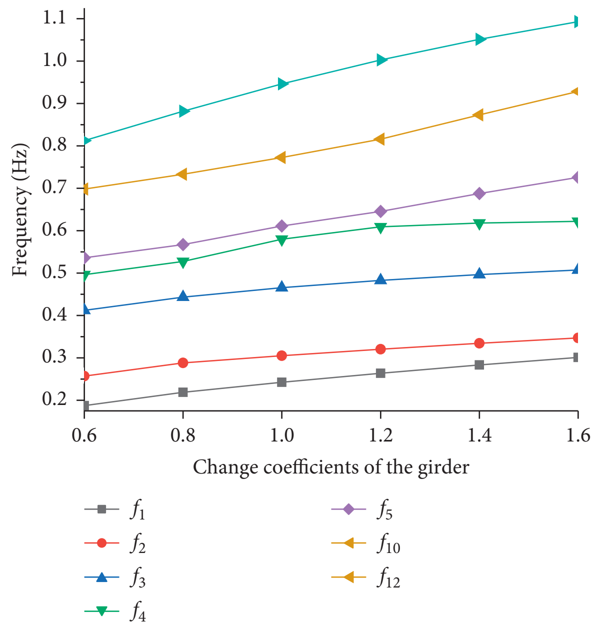

(a)

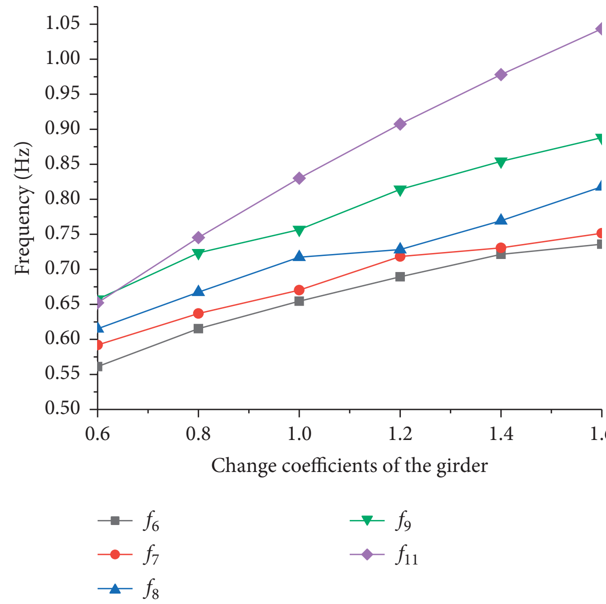

(b)

Figure 6: Influence of stiffness change coefficient of the girder on bending modes and bending torsion-coupling modes. (a) Bending modes. (b) Bending torsion-coupling modes.

first mode. The increase of the whole vibration mode frequency shows that the bending and torsional coupling ability of the bridge can be enhanced by improving the stiffness of the girder. The rise of the modal frequency of dynamic analysis means the enhancement of bridge dynamic characteristics. The cable-stayed bridge is an integral structure connecting pylon, stayed cable, and girder. Because the stayed cable pulls the girder and the girder is connected with the pylon, the overall stiffness can be improved after the stiffness of the girder is increased. The improvement of overall stiffness will lead to the improvement of dynamic performance. Improving the stiffness of the main girder can greatly enhance the dynamic characteristics of the bridge, which means that the stiffness of the main girder can improve the wind resistance and seismic resistance of the bridge. There are many measures to improve the stiffness of the main girder, such as replacing the steel with stronger rigidity, increasing the members, and using stronger connection devices.

6.2.2. The Stiffness of Stayed Cables. As shown in Figure 7, the stiffness of other components is kept unchanged, the stiffness change coefficient of the stayed cables is set to 0.6, 0.8, 1.2, 1.4, and 1.6, and the bending modes and bending torsion-coupling modes are compared and studied. It is found that the change of the stiffness of the stayed cables has some influence on the mode shape of the bridge.

It can be seen from Figure 7 that when the cable stiffness coefficient is 0.8, the first 12 main mode frequencies have a sudden drop. The reason is that when the cable stiffness coefficient is 0.8, the first-order vertical bending of the main span of the girder appears at the fundamental frequency mode (as is shown in Figure 8), while when the cable stiffness coefficient is 1.0, 1.2, 1.4, and 1.6, the first-order vertical bending of the main span of the girder appears at the fundamental frequency mode. Excluding the special case of the cable stiffness coefficient of 0.8, with the stiffness coefficient of the cable rising from 0.6 to 1.6, the rising rates of the bending modes and bending torsion-coupling modes are very low. The lowest rising rate is the frequency of the 7th-order mode, less than 1%. The median rate of increase is less than 5%. From the original design as a benchmark, the change in cable stiffness has a more complicated impact on the dynamic characteristics of the bridge. When the stiffness of the cable drops from the benchmark, the dynamic characteristics of the bridge may change significantly. Therefore, adjusting the stiffness of the cables in the design of the bridge may have a greater impact on the dynamic characteristics of the bridge, thereby affecting the seismic stability and wind-resistant of the bridge.

6.2.3. The Stiffness of Pylon. As shown in Figure 9, the stiffness of other members was kept unchanged, the stiffness change coefficient of the pylons was changed to 0.6, 0.8, 1.0, 1.2, 1.4, and 1.6, and the bending modes and bending torsion-coupling modes are compared and studied. It is found that the change of pylon stiffness will not affect the mode shape of the bridge.

It can be seen from Figure 9 that with the stiffness coefficient of the pylons rising from 0.6 to 1.6, the frequency of the first 12 modes of the bridge shows an upward trend. For bending modes, when the stiffness coefficient increases from 0.6 to 1.6, the frequency of the 3rd-order mode has the largest rising rate, reaching 23.5%, and the lowest rising rate is 9.8% at the 10th-order mode. However, it should be noted that when

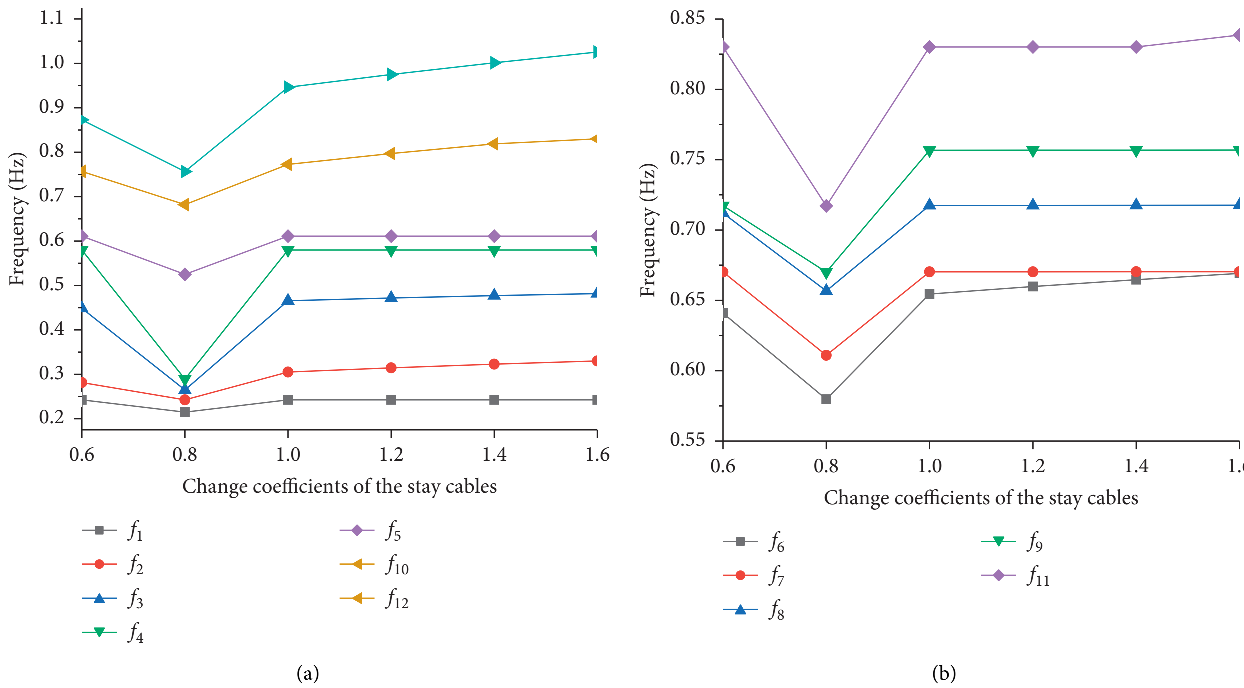

FIGURE 7: Influence of stiffness change coefficient of the stayed cables on bending modes and bending torsion-coupling modes. (a) Bending modes. (b) Bending torsion-coupling modes.

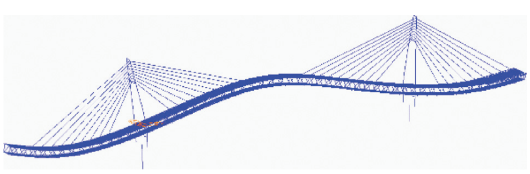

FIGURE 8: The modal shape of the fundamental frequency with the stiffness coefficient of 0.8.

the stiffness coefficient of the pylons is increased from 1 to 1.2, 1.4, and 1.6, the frequency rising rate is very low, and the frequency of the 2nd-order mode has the largest rising rate, which is only 4.2%. This shows that the stiffness of C50 concrete pylon is enough, and the dynamic performance will be weakened if it is reduced. The law of bending torsion-coupling mode is different from that of bending torsion-coupling mode. For bending torsion-coupling mode, when the pylon stiffness coefficient is increased from 1 to 1.2, 1.4, and 1.6, the rising rate of modal frequency is not small. The lowest rate of increase was 6.2%, and the highest rate was 10.8%. This shows that when the pylon stiffness increases, although it cannot improve the overall bending strength of the bridge, it is helpful for the torsional strength. Adjusting the stiffness of the pylon will have some impact on the seismic stability and wind-resistant of the bridge. The stiffness of the pylon can be appropriately increased in the design of the bridge to improve the seismic stability and wind-resistant of the bridge.

6.2.4. Concentration of the Dead Load in the Girder. Through the observation of the mode shape of the bridge after the change of the concentration of the dead load, it was found that the change of the concentration of the dead load did not affect the mode shape of the bridge. The change coefficients are set as 0.6, 0.8, 1.0, 1.2, 1.4, and 1.6, respectively. As shown in Figure 10, the bending modes and bending torsion-coupling modes are compared and studied.

It can be seen from Figure 10 that with the concentration of the dead load coefficient increasing from 0.6 to 1.6, the frequencies of the first 12 modes of the bridge show a downward trend. For bending modes, the frequency of the 1st-order mode with the highest drop rate is 21.6%, and the lowest one is 14.1% in the 10th-order mode. For bending torsion-coupling modes, the largest descending rate is the 6th-order mode, which reaches 20.6%, and the frequency of the 8th-order mode has the smallest descending rate, reaching 10.4%. The increase of the concentration of the dead load is unfavorable to the bending and torsion resistance of the bridge. When the dead load concentration increases, the bridge needs to bear more loads, which will lead to the decline of dynamic performance. In order to ensure the seismic stability and wind-resistant of the bridge, reasonable light materials should be selected as the second-stage dead load of the bridge.

6.2.5. Number and Location of Auxiliary Piers. As is shown in Figure 11, the location and number of auxiliary piers will not affect the basic frequency of the bridge. The number of auxiliary piers is set from 1 to 6. Because the left span of the bridge is larger than the right span, one auxiliary pier is set in the left-side span when the number of auxiliary piers is 1. When the number of auxiliary piers is 2, one auxiliary pier is set in the left-side and right-side spans, respectively. When the number is 3, two auxiliary piers are set in the left-side

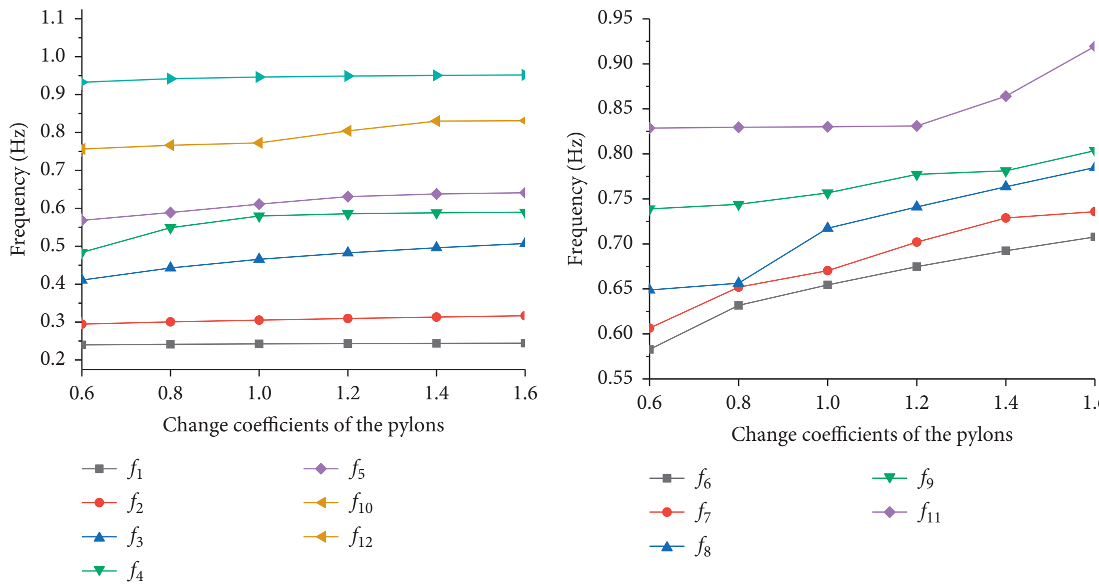

(a) (b)

Figure 9: Influence of stiffness change coefficient of the pylons on bending modes and bending torsion-coupling modes. (a) Bending modes. (b) Bending torsion-coupling modes.

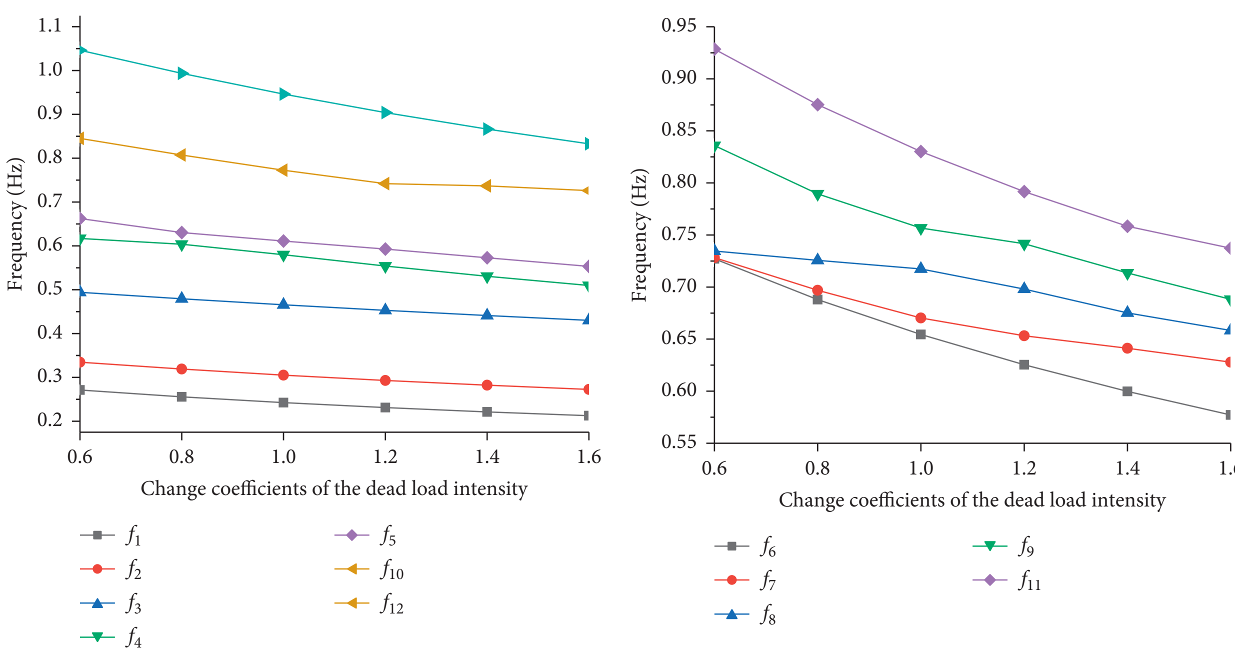

(a) (b)

Figure 10: Influence of change of the concentration of the dead load on bending modes and bending torsion-coupling modes. (a) Bending modes. (b) Bending torsion-coupling modes.

span and one auxiliary pier is set in the right-side span, and so on. As is shown in Figure 12, the influence of the number of auxiliary piers on the dynamic characteristics of the bridge was studied.

It can be seen from Figure 12 that with the number of auxiliary piers increasing from 0 to 6, the frequencies of the first 12 modes of the bridge show an upward trend. For bending modes, when the auxiliary pier increases from 0 to 2, the frequencies increase obviously, the maximum is the 12th mode, reaching 23.4%. However, when it increases from 2 to 3, 4, 5, and 6, the rising rate is low, and the maximum is the 12th-order mode, which is only 7.4%. The law of bending torsion-coupling mode is similar to that of bending mode. When the number of auxiliary piers is more

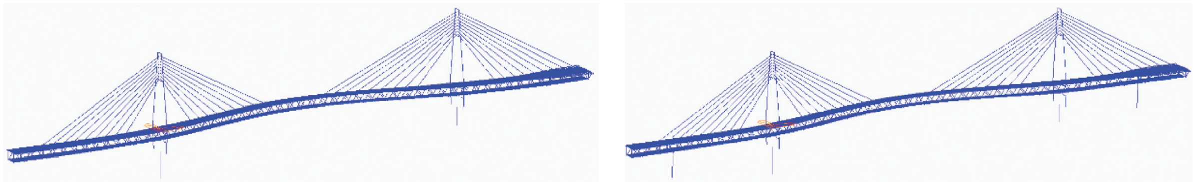

(a) (b)

Figure 11: The 1st-order mode shape comparison of a cable-stayed bridge with and without auxiliary piers. (a) The shape of 1st-order mode of a cable-stayed bridge without auxiliary piers. (b) The shape of 1st-order mode cable-stayed bridge with auxiliary piers.

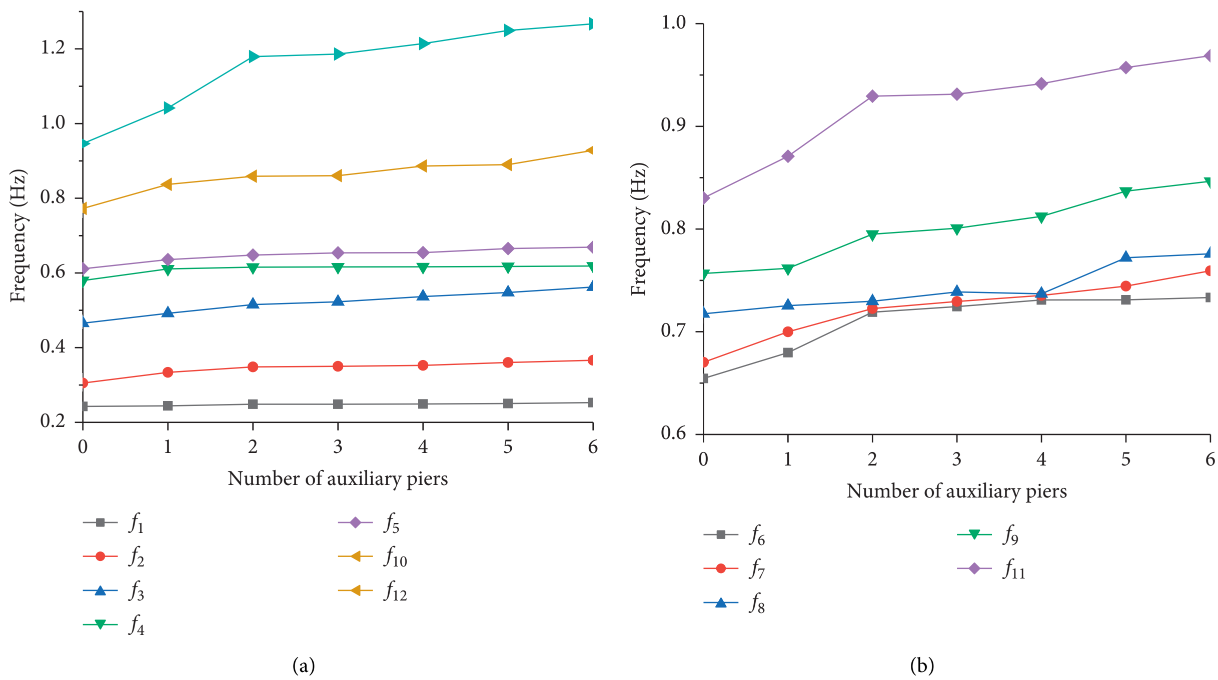

Figure 12: Influence of the number of auxiliary piers on bending modes and bending torsion-coupling modes. (a) Bending modes. (b) Bending torsion-coupling modes.

than 2, the frequency rise is small. Therefore, the installation of auxiliary piers on the double-pylon cable-stayed bridge with a single-cable plane and steel truss girder can improve its bending and torsion resistance, which is beneficial to the seismic stability and wind-resistant of the bridge. In the bridge design, the stability of the bridge can be strengthened by adding auxiliary piers. However, when the number of auxiliary piers is greater than 2, the increase of frequency of each vibration mode is limited.

6.2.6. Structural System of Girder and Pylon. The structural system of a double-pylon cable-stayed bridge usually includes the rigid frame system, semifloating system, pylon and girder consolidation system, and floating system. Several systems of double-pylon cable-stayed bridges are shown in Figure 13. The influence of structural system changes on the bending mode and bending torsion-coupling mode is shown in Figure 14.

It can be seen from Figure 14 that the first 12 modal frequencies of the four structural systems are not consistent. The frequencies of the semifloating system and the pylon and girder consolidation system are relatively high, and the frequencies of the floating system and the rigid frame system are relatively low. Because there is no connection between the pylon and girder of the floating system, and the whole girder is floating in the air except for the support at both ends, the dynamic characteristics of the floating system are unstable. On the one hand, the pylons and girder of the rigid frame system are consolidated, the pylon and girder form a whole, the number of indeterminate increases, and the uncertainty factors increase at the same time. On the other hand, if the flexibility of the tower is not enough, the dynamic characteristics of the rigid frame system may become unstable. For the pylon and girder consolidation system and semifloating system, there is a certain connection between the pylon and the girder, but not consolidation. The interaction between the pylons and the girder is smaller than that of the rigid frame system but larger than that of the floating system. Therefore, the dynamic characteristics of the semifloating system and pylon and girder consolidation system are relatively stable.

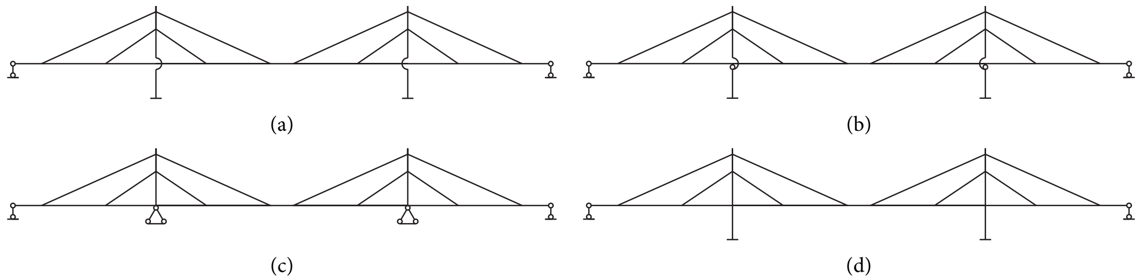

Figure 13: Several systems of the double-pylon cable-stayed bridges. (a) The floating system. (b) The semifloating system. (c) The pylon and girder consolidation system. (d) The rigid frame system.

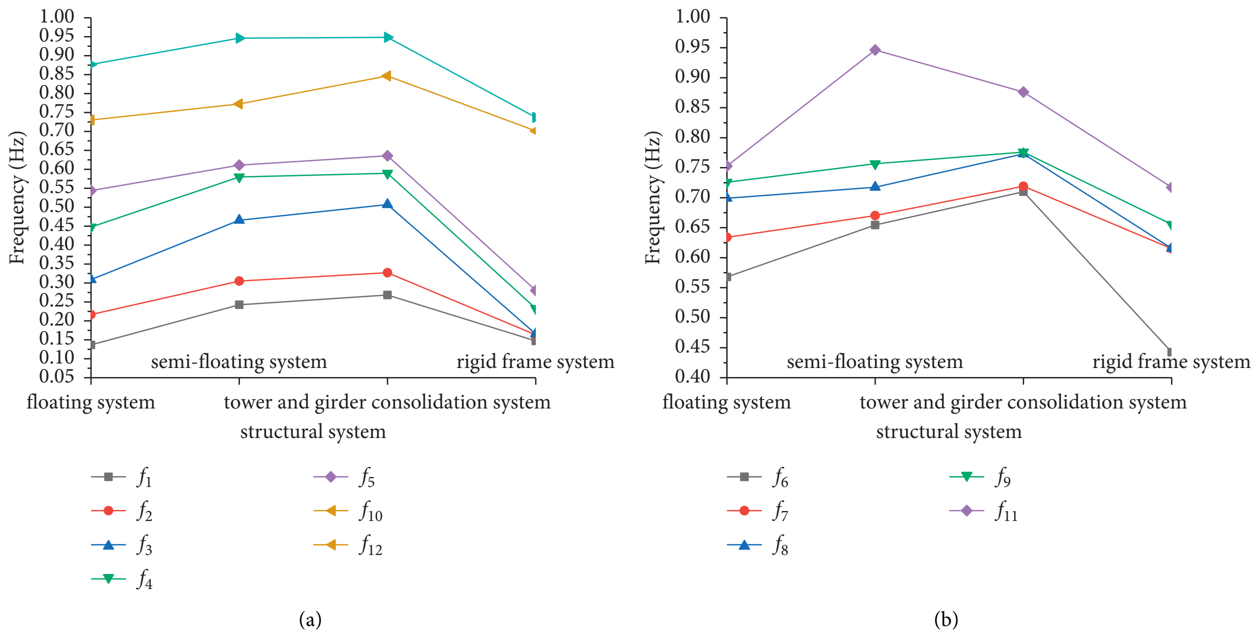

Figure 14: Influence of the changes of the structural system on bending modes and bending torsion-coupling modes. (a) Bending modes. (b) Bending torsion-coupling modes.

7. Conclusions

The double-pylon cable-stayed bridge with single-cable plane and steel truss girder has the feature of novel bridge type, complex structure, and uncertain dynamic characteristics. The dynamic load test was done and the correctness of the FE model was verified. The influence of different stayed cable surface arrangement, girder stiffness, cable stiffness, pylon stiffness, the concentration of the dead load, number of auxiliary piers, and structural system on the dynamic characteristics of the double-pylon cable-stayed bridge with single-cable plane and steel truss girder was analyzed. The conclusion is as follows:

(1) The bending and torsion rigidities of the double-pylon cable-stayed bridge with a single-cable plane and steel truss girder are relatively balanced and weak, which is unfavorable to the wind-resistant of the bridge. However, due to its semifloating system, the seismic responsibility is relatively improved. By changing the single-cable plane layout to the double-cable plane layout, the torsional stiffness of the double-pylon cable-stayed bridge with steel truss girder is improved, which can avoid the occurrence of bending and torsion-coupling mode to a certain extent and enhance the wind resistance of the bridge.

(2) The increase of the concentration of the dead load is unfavorable to the bending and torsion resistance of the bridge. In order to enhance the seismic stability and wind-resistant of the bridge, reasonable light materials should be selected as the second-stage dead load of the bridge.

(3) Adjusting the stiffness of the pylon and girder will affect the seismic stability and wind-resistant of the bridge, and improving the stiffness of the pylon and girder can increase the seismic stability and wind-resistant of the bridge. The change of cable stiffness has a complex influence on the dynamic characteristics of the bridge. When the cable stiffness is 0.8

times of the original structure, the mode shape of the bridge changes greatly. Therefore, adjusting the cable stiffness in the bridge design may have a great impact on the seismic stability and wind-resistant of the bridge.

(4) The installation of auxiliary piers on the double-pylon cable-stayed bridge with a single-cable plane and steel truss girder can improve its bending and torsion resistance, which is beneficial to the seismic stability and wind-resistant of the bridge. In the bridge design, the stability of the bridge can be strengthened by adding auxiliary piers.

(5) The dynamic characteristics of the floating system and the rigid frame system are unstable, while the dynamic characteristics of the semifloating system and the pylon and girder consolidation system are better. The semifloating system or the pylon and girder consolidation system should be used in the follow-up similar bridges.

Data Availability

The data used to support the findings of this study are included within the article.

Conflicts of Interest

The authors declare that there are no conflicts of interest regarding the publication of this paper.

Acknowledgments

The authors appreciate the financial support from the Natural Science Foundation of PR China (51908093), State Key Laboratory of Mountain Bridge, Tunnel Engineering Development Fund (CQSLBF−Y14, CQSLBF−Y16−10), and Chongqing Returned Overseas Students' Entrepreneurship and Innovation Support Fund (cx2018113 and cx2020117).

References

[1] D. H. Yang, T. H. Yi, and H. N. Li, "Train-induced dynamic behavior analysis of longitudinal girder in cable-stayed bridge," *Smart Structures and Systems*, vol. 21, no. 5, pp. 549–559, 2018.

[2] B. Jian, Y. Su, and M. Li, "Buffeting Response of cable-stayed Bridge during Construction under Skew Winds and Pylon Interference," *KSCE J Civ Eng*, vol. 24, no. 10, pp. 2971–2979, 2020.

[3] Y. Lu, L. Mao, and P. Woodward, "Frequency characteristics of railway bridge response to moving trains with consideration of train mass," *International Engineering Structures*, vol. 42, pp. 9–22, 2021.

[4] N. Deng, "Study on dynamic characteristics of train-bridge coupling based on wireless sensor network," *Journal of Internet Technology*, vol. 20, no. 2, pp. 555–562, 2019.

[5] D. Kuchárová and J. Melcer, "Identification of some dynamic characteristics of a bridge structure," *Procedia Engineering*, vol. 190, pp. 304–309, 2017.

[6] Y. Ni, Q. W. Zhang, and J. F. Liu, "Dynamic property evaluation of a long-span cable-stayed bridge (sutong bridge) by a bayesian method," *International Journal of Structural Stability and Dynamics*, vol. 19, no. 1, Article ID 1940010, 2019.

[7] J. Guo and J.-X. He, "Dynamic response analysis of ship-bridge collisions experiment," *Journal of Zhejiang University-SCIENCE*, vol. 21, no. 7, pp. 525–534, 2020.

[8] D. M. Siringoringo and Y. Fujino, "Dynamic characteristics of a curved cable-stayed bridge identified from strong motion records," *Engineering Structures*, vol. 29, no. 8, pp. 2001–2017, 2007.

[9] Y. Li, S. Y. Zhu, C. S. Cai, and C. Yang, "Dynamic response of railway vehicles running on long-span cable-stayed bridge under uniform seismic excitations," *International Journal of Structural Stability and Dynamics*, vol. 16, no. 5, Article ID 1550005, 2016.

[10] A. Bayraktar, A. C. Altunişik, B. Sevim, T. Türker, A. Domaniç, and Y. Taş, "Vibration characteristics of kömürhan highway bridge constructed with balanced cantilever method," *Journal of Performance of Constructed Facilities*, vol. 23, no. 2, pp. 90–99, 2009.

[11] A. Bayraktar, A. C. Altunişik, B. Sevim, and T. Ş. Özşahin, "Environmental effects on the dynamic characteristics of the Gülburnu Highway Bridge," *Civil Engineering and Environmental Systems*, vol. 31, no. 4, pp. 347–366, 2014.

[12] B. Huang, R. F. Seresh, and L. Zhu, "Statistical analysis of basic dynamic characteristics of large span cable-stayed bridge based on high order perturbation stochastic fem," *Advances in Structural Engineering*, vol. 16, no. 9, pp. 1499–1512, 2013.

[13] N. A. Londono, D. T. Lau, and M. Rahman, "Characteristics of dynamic monitoring data and observed behavior of the Confederation Bridge due to operational load variations," *Canadian Journal of Civil Engineering*, vol. 40, no. 2, pp. 393–409, 2013.

[14] H. Cai and H. Lu, "Dynamic response of long-span continuous curved box girder bridge under seismic excitation," *Journal of Vibroengineering*, vol. 21, no. 3, pp. 696–709, 2019.

[15] X. H. He, B. Wei, Y. F. Zou, and D. Y. Hu, "Dynamic characteristics and seismic response analysis of a long-span steel-box basket-handle railway arch bridge," *Journal of Vibroengineering*, vol. 17, no. 5, pp. 2422–2432, 2015.

[16] D. Wang, Y. Deng, and Y. Liu, "Influence of central buckle on suspension bridge dynamic characteristics and driving comfort," *Journal of Central South University*, vol. 22, no. 8, pp. 3108–3115, 2015.

[17] H. Wang, G. Zou, Q. Li, and K. Jiao, "Parameter effects on the dynamic characteristics of a super-long-span triple-tower suspension bridge," *Journal of Zhejiang University - Science*, vol. 11, no. 5, pp. 305–316, 2010.

[18] L. Jiang, Y. Feng, W. Zhou, and B. He, "Vibration characteristic analysis of high-speed railway simply supported beam bridge-track structure system," *Steel and Composite Structures*, vol. 31, no. 6, pp. 591–600, 2019.

[19] A. Plotnikova, L. Wotherspoon, S. Beskhyroun, and Z. Yang, "Influence of seasonal freezing on dynamic bridge characteristics using in-situ monitoring data," *Cold Regions Science and Technology*, vol. 160, pp. 184–193, 2019.

[20] Z.-H. Zhu, W. Gong, K. Wang, Y. Liu, M. T. Davidson, and L.-Z. Jiang, "Dynamic effect of heavy-haul train on seismic response of railway cable-stayed bridge," *Journal of Central South University*, vol. 27, no. 7, pp. 1939–1955, 2020.

[21] F. Geng, Y. Ding, H. Xie, J. Song, and W. Li, "Influence of structural system measures on the dynamic characteristics of a multi-span cable-stayed bridge," *Structural Engineering & Mechanics*, vol. 52, no. 1, pp. 51–73, 2014.

[22] G.-P Zhou, A.-Q Li, J.-H Li, and M.-J Duan, "Test and numerical investigations on static and dynamic characteristics of extra-wide concrete self-anchored suspension bridge under vehicle loads," *Journal of Central South University*, vol. 24, no. 10, pp. 2382–2395, 2017.

[23] C. E. Ventura, A. J. felber, and S. F. Stiemer, "Determination of the dynamic characteristics of the Colquitz River Bridge by full-scale testing," *Canadian Journal of Civil Engineering*, vol. 23, no. 2, pp. 536–548, 1996.

[24] S. S. Roy and S. R. Dash, "Dynamic behavior of the multi span continuous girder bridge with isolation bearings," *International Journal of Bridge Engineering (IJBE)*, vol. 6, no. 2, pp. 01–23, 2018.

[25] X. Xie, X. Li, and Y. Shen, "Static and dynamic characteristics of a long-span cable-stayed bridge with CFRP cables," *Materials*, vol. 7, no. 6, pp. 4854–4877, 2014.

[26] C. Casalegno and S. Russo, "Dynamic characterization of an all-FRP bridge," *Mechanics of Composite Materials*, vol. 53, no. 1, pp. 17–30, 2014.

[27] E. Chen, X. Zhang, and G. Wang, "Rigid-flexible coupled dynamic response of steel-concrete bridges on expressways considering vehicle-road-bridge interaction," *Advances in Structural Engineering*, vol. 23, no. 1, pp. 160–173, 2020, https://doi.org/10.1177/136 9433219866092.

[28] X. J. Che, "Simulation modeling of dynamic characteristics of sea crossing bridge under wind invasion," *Journal of Coastal Research*, vol. 83, pp. 93–97, 2020, https://doi.org/10.2112/SI83-016.1.

[29] I. Paeglite, J. Smirnovs, and A. Paeglitis, "Evaluation of the increased dynamic effects on the highway bridge superstructure," *The Baltic Journal of Road and Bridge Engineering*, vol. 13, no. 3, pp. 301–312, 2018.

[30] M. Vospernig and M. Reiterer, "Evaluierung der dynamischen Systemeigenschaften von einfeldrigen Stahlbeton-Eisenbahnbrücken," *Beton- und Stahlbetonbau*, vol. 115, no. 6, pp. 424–437, 2020, https://doi.org/10.1002/best.201900093.

[31] J.-H. Park, T.-C. Huynh, K.-S. Lee, and J. T. Kim, "Wind and traffic-induced variation of dynamic characteristics of a cable-stayed bridge - benchmark study," *Smart Structures and Systems*, vol. 17, no. 3, pp. 491–522, 2016.

[32] HY. Gou, B. Yang, and W. Guo, "Static and dynamic responses of a tied-arch railway bridge under train load," *Structural Engineering & Mechanics*, vol. 71, no. 1, pp. 13–22, 2019.

[33] H. Y. Gou, C. Liu, W. Zhou, and Y. Bao, "Dynamic responses of a high-speed train passing a deformed bridge using a vehicle-track-bridge coupled model," *Proceedings of the Institution of Mechanical Engineers - Part F: Journal Of Rail And Rapid Transit*, vol. 235, no. 4, pp. 463–477, 2020.

[34] Y. Li, Y. Bao, and S. Dong, "Impact Coefficient Analysis of Long-Span Railway Cable-Stayed Bridge Based on Coupled Vehicle-Bridge Vibration," *Shock and Vibration*, vol. 2016, 2016 https://doi.org/10.1155/2015/641731, Article ID 641731.

[35] G. Min, X. Liu, and C. Wu, "Influences of two calculation methods about dynamic tension on vibration characteristics of cable-bridge coupling model," *Discrete Dynamics in Nature and Society*, vol. 2021, Article ID 6681954, 2021.

[36] P. Gorski, M. Napieraj, and E. Konopka, "Variability evaluation of dynamic characteristics of highway steel bridge based on daily traffic-induced vibrations," *Measurement*, vol. 164, Article ID 108074, 2020.

[37] F. Han, D.-H Dan, and H. Wang, "A study on dynamic amplification factor and structure parameter of bridge deck pavement based on bridge deck pavement roughness," *Advances in Civil Engineering*, vol. 2018, 2018 https://doi.org/10.115 5/2018/9810461, Article ID 9810461.